

pyTFM: A tool for Traction Force and Monolayer Stress Microscopy

Andreas Bauer^{1*}, Magdalena Prechová^{2*}, Martin Gregor^{2*}, Ben Fabry¹

1 Department of Physics, Friedrich-Alexander University Erlangen-Nürnberg, Erlangen, Germany

2 Laboratory of Integrative Biology, Institute of Molecular Genetics of the Czech Academy of Sciences, Prague, Czech Republic

* andreas.b.bauer@fau.de

Abstract

Cellular force generation and force transduction are of fundamental importance for numerous biological processes and can be studied with the methods of Traction Force Microscopy (TFM) and Monolayer Stress Microscopy. Traction Force Microscopy and Monolayer Stress Microscopy solve the inverse problem of reconstructing cell-matrix tractions and inter- and intra-cellular stresses from the measured cell force-induced deformations of an adhesive substrate with known elasticity. Although several laboratories have developed software for Traction Force Microscopy and Monolayer Stress Microscopy computations, there is currently no software package available that allows non-expert users to perform a full evaluation of such experiments. Here we present pyTFM, a tool to perform Traction Force Microscopy and Monolayer Stress Microscopy on single cells, cell patches and cell layers grown in a 2-dimensional environment. pyTFM was optimized for ease-of-use; it is open-source and well documented (hosted at <https://pytfm.readthedocs.io/>) including usage examples and explanations of the theoretical background. pyTFM can be used as a standalone Python package or as an add-on to the image annotation tool *ClickPoints*. In combination with the *ClickPoints* environment, pyTFM allows the user to set all

necessary analysis parameters, select regions of interest, examine the input data and intermediary results, and calculate a wide range of parameters describing forces, stresses, and their distribution. The Monolayer Stress Microscopy implementation in pyTFM allows for the analysis of small cell patches and single cells; we analyze the accuracy and performance of Traction Force Microscopy and Monolayer Stress Microscopy algorithms using synthetic and experimental data from epithelial cell patches.

1 Introduction

The generation of active forces gives cells the ability to sense the mechanical properties of their surroundings [1], which in turn can determine the cell fate during differentiation processes [2], the migratory behavior of cells [3] or the response to drugs [4].

Measuring cellular force generation is important for understanding fundamental biological processes including wound healing [5], tissue development [6], metastasis formation [7, 8] and cell migration [3].

Cellular forces can be divided into three categories: Forces that are transmitted between a cell and its surrounding matrix (also referred to as traction forces), forces that are transmitted between cells, and forces that are transmitted inside cells.

Traction forces can be measured with Traction Force Microscopy (TFM), which is most easily applied to cells grown in a 2-dimensional environment: Cells are seeded on a planar elastic substrate on which they adhere, spread, and exert forces. The substrate contains fiducial markers such as fluorescent beads for tracking cell force-induced deformations of the substrate. Typically, the substrate is imaged in a tensed and a relaxed (force-free) state, whereby force relaxation is achieved by detaching the cells from the substrate. These two images are then compared to quantify substrate deformations, either by tracking each individual marker bead, or more commonly, by cross-correlation based Particle Image Velocimetry (PIV) [9].

The deformation field of the substrate is subsequently analyzed to calculate the cell-generated tractions in x- and y-directions. (Note that if the substrate deformations in z-direction are also measured, which requires at least one additional image taken at a different focal plane, it is possible to compute the tractions in z-direction [10]. In what follows, however, we ignore deformations and tractions in z-direction.) The calculation

of the traction field from the deformation field is an inverse problem for which a number
25 of algorithms have been developed, including numerical methods [11, 12], Fourier-based
26 deconvolution [13], and Finite Element (FE) computations [14], all of which have
27 specific advantages and disadvantages (see Sabass et al. 2007 [15] for a detailed
28 discussion). pyTFM uses the Fourier Transform Traction Cytometry (FTTC) algorithm
29 [13], as it is computationally fast and does not require the location of the cell boundary
30 as an additional input.
31

Tractions must be balanced by forces transmitted within or between cells. These
32 forces are usually described by stress tensors. The stress tensor field for cells grown in a
33 2-dimensional environment can be calculated using the Monolayer Stress Microscopy
34 method [16, 17], whereby the cell or cell patch is modeled as an elastically stretched
35 2-dimensional sheet with point-like contacts to the matrix so that the tractions are
36 balanced by the internal stress of the elastic sheet.
37

In pyTFM, the cell or cell patch is modelled as a linear elastic sheet represented by a
38 network of nodes and vertices so that the stresses can be calculated by a standard
39 two-dimensional Finite Element Method (FEM). First, forces with the same magnitude
40 but opposing direction to the local tractions are applied to each node. Then, internal
41 strains and consequently stresses are calculated based on the network geometry and
42 elastic properties.
43

pyTFM uses the Monolayer Stress Microscopy algorithm developed by Tambe et al.
44 2013 [17]. In this implementation, the calculated network strain has no physical
45 meaning, as the matrix strain and the cell strain are not required to match [18].
46 Consequently, the Young's modulus of the elastic sheet has no influence on the stress
47 estimation, and the Poisson's ratio has only a negligible influence. Both parameters can
48 therefore be freely chosen [17]. Note that there are different implementations of
49 Monolayer Stress Microscopy in which cell and matrix deformations are coupled and the
50 network elasticity corresponds to the effective cell elasticity, which must be known to
51 obtain correct results [19]. A comparison about these two approaches can be found in
52 [18].
53

pyTFM uses a modified Monolayer Stress Microscopy algorithm for small cell
54 patches. Stress microscopy for single cells and small cell patches suffers from the low
55 spatial resolution of the TFM algorithm. A significant part of the tractions can seem to
56

originate from outside the cell area, and when only tractions beneath the cell area are
57 considered, the stress field is underestimated. This problem cannot be remedied by
58 constraining the tractions to be zero outside the cell area (constrained TFM) as this
59 tends to produce large spurious tractions at the cell perimeter [13] and hence
60 unphysically high stresses in the cell monolayer. Ng et al. 2014 [20] addressed this issue
61 by expanding the FEM-grid to cover all tractions generated by the cell patch and by
62 exponentially decreasing the stiffness of the FEM-grid with increasing distance to the
63 cell patch edge. In our implementation, the FEM-grid is also expanded to cover all
64 cell-generated tractions, however, we found it unnecessary to introduce a stiffness
65 gradient in the FEM-grid. Moreover, zero-translation and zero-rotation constraints are
66 explicitly added to the FEM-algorithm in pyTFM.
67

Finally, pyTFM adds a number user-friendly features to easily set parameters, select
68 regions of interest and quickly evaluate results. For this, pyTFM can be optionally used
69 as an add-on to the image annotation tool *ClickPoints* [21]. This makes the analysis of
70 large data sets particularly easy by sorting input and output data in a database and
71 allowing the user to browse through it.
72

pyTFM is well documented, including detailed usage examples, information on the
73 theory of TFM and Monolayer Stress Microscopy, and explanations about the calculated
74 parameters. The documentation is hosted at <https://pytfm.readthedocs.io>.
75

2 Design and implementation

pyTFM is a Python package implemented in Python 3.6. It is mainly intended to be
77 used as an add-on for the image display and annotation tool *ClickPoints*, but can also
78 be used as a stand-alone Python library.
79

pyTFM performs TFM and Monolayer Stress Microscopy following the workflow
80 shown in Fig. 1A. The main steps of the workflow are the calculation of the
81 deformation field from images of the cell substrate in a tensed and relaxed state, the
82 calculation of the traction field, and the calculation of the monolayer stress field. The
83 mathematical details of these steps are discussed in Section 2.2. Deformation, traction
84 and stress fields are further analyzed to extract scalar measures of cellular stress, force
85 generation, and force transduction between cells.
86

Fig 1. Workflow of pyTFM and image database organization. A: Workflow of TFM and Monolayer Stress Microscopy analysis with pyTFM. B: Organization of the pyTFM *ClickPoints* database. Input images are colored in orange, intermediary results in yellow, and the final output in the form of scalar measures in green. The mask that defines the cell boundaries and the area over which strain energy, contractility and monolayer stresses are computed is colored light blue.

Cellular force generation is quantified by the total force generation and centripetal contractility. Total force generation in turn is described by the strain energy that is elastically stored in the substrate, and centripetal contractility is described by the sum of all cell-generated forces projected towards a single force epicenter. Stresses are quantified by average normal and shear stresses and their coefficient of variation, which is a measure for stress fluctuations. Cell-cell force transduction is quantified by the line tension, which is the force per unit length acting on a segment of a cell-cell boundary. Specifically, pyTFM calculates the average magnitude of the line tension as well as the average normal and shear component of the line tension. Additionally, pyTFM calculates the area and number of cells of each cell patch, which can be used to normalize the quantities above. We provide more details on how these quantities are defined and how to interpret them in the Supplementary S1 File.

The user is required to select an area of the traction field over which the strain energy, contractility and monolayer stresses are computed. This area should cover all cell-generated tractions and is thus typically larger than the cell area. However, a significant further extension of the user-selected area beyond the cell edge will lead to an underestimation of monolayer stresses, as will be further discussed in Section 2.2.2. Optionally, the outline of the cell or cell patch can be selected, defining the area over which average stresses and stress fluctuations are computed. Also optionally, the outline of cell-cell boundaries can be selected to calculate force transduction between cells.

pyTFM generates several output files. All fields (deformations, tractions, stresses) are saved in the form of NumPy arrays as binary .npy files and are plotted as vector fields or heat maps. The cell-cell force transduction and the strain energy density can also be plotted (see Fig. 5 for an example). The user has full control over which plots are produced. All calculated scalar results are saved in a tab-separated text file. pyTFM includes Python functions to read, compare and statistically analyze the result text files of several experiments. Alternatively, the result text files can be opened with

standard text editors or data analysis tools such as Excel.

114

2.1 Integration of pyTFM with *ClickPoints* databases

115

When using the pyTFM add-on in *ClickPoints*, input and output images are organized
116 in a database (Fig. 1B), which allows users to efficiently navigate large data sets. The
117 database is organized in frames and layers: Each frame represents one field of view.
118 Initially, three layers are assigned to each frame. These layers contain images of the
119 substrate in the tensed and relaxed state, and an image of the cells. Output plots such
120 as the deformation field or the traction field are added as new layers in each analysis
121 step. Additionally, each frame is associated with a mask object in the form of an integer
122 array representing the user selected areas and cell outlines. This mask object can be
123 drawn directly in *ClickPoints* and can be displayed in each layer of a frame.
124

125

pyTFM provides a graphical user interface for the *ClickPoints* environment, which
126 allows the user to select input images, to set all relevant analysis parameters (e.g. the
127 elasticity of the substrate), and to select whether the analysis should be performed on
128 all frames or just the currently viewed frame (Fig. 2). A number of tools are provided
129 by *ClickPoints*, e.g. to draw masks, to adjust contrast and brightness of the displayed
130 images, to measure distances and object sizes, and to export images and video
131 sequences.

132

Fig 2. User interface of pyTFM. 1: Check boxes to select specific analysis steps. 2:
133 Selection of input images, drift correction and semi automatic segmentation of cell
134 borders. 3: Drop-down menu to select between analysing all frames in a database or
135 analysing only the currently viewed frame. 4: Parameters for PIV and TFM. 5:
136 User-selected region (red outline) and cell boundaries (green) for computing tractions,
137 stresses, contractility, strain energy and line tensions. 6: *ClickPoints* tools to select the
138 region and the cell boundaries by drawing masks. 7: *ClickPoints* navigation bar
139 through frames. Layers are navigate with the Page Up and Page Down keys, and frames
140 are navigated with the left and right arrow keys. 8: *ClickPoints* panel to adjust contrast
141 and brightness of the image display. This is helpful for manually segmenting cell
142 borders.

2.2 Implementation of TFM and Monolayer Stress Microscopy 132

2.2.1 Deformation fields and TFM 133

Deformation fields are calculated from the images of the substrate in a tensed and 134
relaxed state using the cross correlation-based Particle Image Velocimetry (PIV) 135
algorithm implemented in the openPIV Python package [9]. PIV is performed by 136
selecting for example a 50x50 pixel tile around a given pixel from the tensed image and 137
shifting the tile by pixel increments in all directions across the corresponding tile in the 138
relaxed image. This yields a correlation matrix of in this case 99x99 pixels. The 139
deformation vector is then obtained by calculating the vector between the position of 140
the highest correlation and the center of the matrix. The initial deformation vector is 141
further refined to sub-pixel accurate values by fitting a 2D Gauss curve to the directly 142
neighbouring correlation values. To reduce noise, deformation vectors with a 143
signal-to-noise ratio smaller than 1.03 are exclude and replaced by the local mean of the 144
surrounding deformations at distances ≤ 2 pixel. The signal-to-noise ratio of each 145
deformation vector is defined as the ratio of the correlation of the highest peak and the 146
correlation of the second-highest peak outside of a neighborhood of 2 pixels around the 147
highest peak. The user may also correct a drift between the two input images: The drift 148
is identified by cross-correlating the entire images and then corrected by cropping both 149
images to the common field of view. 150

Tractions are calculated with the Fourier Transform Traction Cytometry (FTTC) 151
method [13]. Deformations (\vec{u}) and tractions (\vec{t}) are related by the convolution of the 152
traction vector field and a Greens tensor K : 153

$$\vec{u} = K \otimes \vec{t} \tag{1}$$

In the case of a linearly elastic semi-infinite substrate, K is given by the Boussinesq 154
equations [22]. Inverting Eq. 1 and solving for the tractions is difficult in real space. 155
However, by exploiting the convolution theorem, the equation simplifies to a 156
multiplication in Fourier space: 157

$$\tilde{\vec{u}}(\vec{k}) = \tilde{K}(\vec{k}) \tilde{\vec{T}}(\vec{k}) \tag{2}$$

where $\tilde{u}(\vec{k})$, $\tilde{T}(\vec{k})$ and $\tilde{K}(\vec{k})$ are the Fourier transforms of the deformation field, the traction field and the Greens tensor. The latter can be found in [13].

Eq. 2 can be analytically solved and thus allows for the direct calculation of tractions in Fourier space. Traction in real space are then obtained by applying the inverse Fourier transform and an additional Gaussian filter with a sigma of typically 1-3 μm .

The original TFM algorithm assumes that the underlying substrate is infinitely thick, which is justified in the case of single cells with dimensions that are smaller than the thickness of the elastic substrate. In the case of cell patches, however, this assumption is inadequate. We have therefore included a correction term for finite substrate thickness [23].

2.2.2 Monolayer Stress Microscopy

Stresses in a cell sheet are calculated with an implementation of Monolayer Stress Microscopy as described in [16, 17]. For computing stresses in small cell patches or single cells, we implemented a method that corrects for the limited spatial resolution of unconstrained TFM, which otherwise would lead to a substantial underestimation of stresses [20]. Details of this correction are described below.

In the absence of inertial forces, tractions and stresses are balanced according to the relation:

$$\begin{aligned} -t_x &= \frac{\delta\sigma_{xx}}{\delta x} + \frac{\delta\sigma_{yx}}{\delta y} \\ -t_y &= \frac{\delta\sigma_{yx}}{\delta x} + \frac{\delta\sigma_{yy}}{\delta y} \end{aligned} \quad (3)$$

where σ_{xx} , σ_{yy} are the normal stresses in x- and y- direction, σ_{yx} is the shear stress, and t_x and t_y are the x- and y-components of the traction vector. This differential equation is solved using a Finite Element method (FEM) where the cell patch is modeled as a 2-dimensional network of nodes arranged in a grid of quadrilateral elements. Each node in the FEM-grid is loaded with a force of the same magnitude but opposing direction as the local tractions. In the standard FE method, the nodal displacements \vec{d} of the cell patch are calculated by solving the equation

$$\vec{d} = K^{-1} \vec{f} \quad (4)$$

where \vec{f} are the vector of nodal forces, and K^{-1} is the inverse stiffness matrix. The 183
nodal displacements are converted to strains by taking the derivative in x- and 184
y-direction. Then, the strain is used to calculate the stress from the stress-strain 185
relationship of a linearly elastic 2-dimensional material: 186

$$\begin{pmatrix} \sigma_{11} \\ \sigma_{22} \\ \sigma_{12} \end{pmatrix} = \frac{E}{1-v^2} \begin{pmatrix} 1 & v & 0 \\ v & 1 & 0 \\ 0 & 0 & 1-v \end{pmatrix} \begin{pmatrix} \epsilon_{11} \\ \epsilon_{22} \\ \epsilon_{12} \end{pmatrix} \quad (5)$$

where E and v are Young's modulus and Poisson's ratio of the material, and ϵ_{11} , ϵ_{22} 187
and ϵ_{12} are the components of the strain tensor. Most of the FEM calculation is 188
performed using the *solidspy* Python package [24]. 189

The stiffness matrix K in Eq. 4 depends on the Young's modulus in such a way that 190
the Young's modulus in Eq. 5 cancels out. The traction-stress relation is therefore 191
independent of the Young's modulus of the cell patch [17]. Furthermore, the Poisson's 192
ratio has only a negligible influence on the stress prediction [17]. In the pyTFM 193
algorithm, the Young's modulus is set to 1 Pa, and the Poisson's ratio is set to 0.5. 194

Eq. 4 is only uniquely solvable if the displacements of at least two nodes of the 195
FEM-grid are assigned (which constrains the solution regarding translation and 196
rotation). In the original Monolayer Stress Microscopy algorithm [17], nodes at the edge 197
of the field of view are constrained to zero displacements in the direction perpendicular 198
to the edge of the field of view. This results in erroneous stresses within a margin of 199
approximately 150 μm to the image edge, which must be excluded from further analysis 200
[17]. This is impractical in the case of small cell patches or single cells. 201

pyTFM addresses this problem by modifying Eq. 4 so that it can be solved without 202
assigning the displacements of boundary nodes. This requires two steps. First, to ensure 203
that all forces and torques of the cell or cell patch are balanced, the forces applied to 204
the FEM-grid are corrected by subtracting the net force and rotating all force vectors to 205
enforce zero torque. Second, equation 4 is constrained to zero force and torque by 206
adding the equations: 207

$$\begin{aligned}\sum(f_x) &= 0 \\ \sum(f_y) &= 0 \\ \sum(f_x r_y - f_y r_x) &= 0\end{aligned}\tag{6}$$

r_x and r_y are the components of the distance vector of the corresponding node to the center of the FEM-grid. Eqs. 6 are equivalent to imposing zero translation and zero rotation constraints. The combined system of Eqs. 6 and Eq. 4 is solved numerically using a standard least-squares minimization.

The analysis of stresses in small cell patches poses a second challenge: The FEM-grid should be of the same size and shape as the cell patch, as outside nodes add additional stiffness, leading to an underestimation of the stress field. However, the limited spatial resolution of both PIV and TFM implies that some forces generated close to the edge of the cell patch are predicted to originate from outside the cell patch (Fig. 4). Neglecting these forces would lead to an underestimation of the stress field. This can be avoided by extending the FEM-grid by a small margin so that all cell-generated forces are included in the analysis. In practice, the user outlines the area with clearly visible tractions (red outline in Fig. 2), over which pyTFM then spans the FEM-grid. We explain further details of this approach in Section 3.1.1.

2.2.3 Limits of applicability of Monolayer Stress Microscopy and TFM

The TFM and Monolayer Stress Microscopy algorithms can only be applied if a number of conditions are met. 2-dimensional TFM relies on the assumption that tractions in z-direction generate only small deformations in the x- and y-plane. This is valid if z-tractions are small, or if the substrate is almost incompressible (Poison's ratio close to 0.5) [11]. Additionally, TFM assumes that the matrix is a linearly elastic material. Both assumptions are valid for polyacrylamide and PDMS, two popular substrates for TFM [25–28].

For Monolayer Stress Microscopy, cells are modeled as a linearly elastic material with uniform elastic properties. As local stiffness inhomogeneities introduce only negligible errors in the stress prediction, it is generally not necessary to consider non-linear elastic effects of the cells [17]. Furthermore, Monolayer Stress Microscopy assumes that the cell

dimensions in the x- and y-plane (length l) is larger the cell height (h). Increased cell 234 height introduces an error in the stress prediction on the order of $(l/h)^2$ [17]. 235

3 Results 236

3.1 Accuracy of TFM and MSM algorithms 237

To evaluate the accuracy of the calculated tractions and stresses, we designed a simple 238 test system with a predefined stress field for which tractions and deformations can be 239 analytically computed. We then compare the analytical solution to the solution 240 provided by pyTFM. 241

The workflow of this test is illustrated in Fig. 3A: First, we define a square-shaped 242 area of $150\text{ }\mu\text{m}$ width representing a cell patch. This area carries a uniform normal 243 stress in x- and y-direction of $1\text{ N}/\mu\text{m}$ magnitude and zero shear stress. Stresses outside 244 the cell patch are set to zero. Next, we calculate the corresponding traction field by 245 taking the spatial derivatives of the stress field and applying Eq. 3. 246

Fig 3. Accuracy of stress and traction force calculation. A: We model a cell 247 colony as a uniformly distributed square-shaped stress field for which we analytically 248 compute a traction field and subsequently a deformation field. We use the deformation 249 field as the input for Traction Force Microscopy and Monolayer Stress Microscopy to 250 recover the traction and the stress fields. B: Input and reconstructed traction field. C: 251 Input and reconstructed stress field. The yellow dashed line shows the extent of the 252 original stress field. D: Contractility and average normal and shear stress and CV for 253 the mean normal stress in the input and reconstructed traction and stress fields. The 254 contractility is computed over an area that is $12\text{ }\mu\text{m}$ larger than the original stress field. 255 Average normal and shear stresses and the CV of the mean normal stress are computed over the area of the original stress field.

From the traction field, we obtain the deformation field by first calculating the 247 Fourier transform of the traction field. Then we use Eq. 2 to obtain the deformation 248 field in Fourier space and, after applying the inverse Fourier transform, in real space. 249 We use a modified Greens Tensor K to account for a finite substrate thickness [23]. The 250 substrate thickness is set to $100\text{ }\mu\text{m}$. 251

The deformation field is then used as the input for the TFM and Monolayer Stress 252 Microscopy algorithms. We use an FEM-grid area that is $5\text{ }\mu\text{m}$ larger than the original 253 stress field area since this resulted in the best stress recovery (Fig. 4A). 254

The computed mean of the normal and shear stresses and the standard deviation of 255

the normal stresses are finally compared with the known input stress (uniform normal
256
stress in x- and y-direction of $1\text{ N}/\mu\text{m}$ magnitude, and zero shear stress). To compare
257
the reconstructed traction field with the analytical solution, we also compute the total
258
contractility (sum of all cell-generated forces projected towards a single force epicenter)
259
over the FEM-grid area.
260

We find that the pyTFM algorithm accurately reconstructs the stress field (Fig. 3B).
261
By contrast, the reconstructed traction field is blurred in comparison to the input
262
traction field (Fig. 3C). This is the effect of a Gaussian smoothing filter with a sigma of
263
 $3\mu\text{m}$ that is applied to the tractions computed by the FTTC algorithm. This filter
264
helps to prevent unphysiological isolated and locally diverging tractions in the case of a
265
noisy input deformation field. In our test case, we do not model the influence of noise
266
and could therefore omit the filter; in practical applications, we find a sigma of $3\mu\text{m}$ to
267
give the best compromise between resolution and noise.
268

The computed average normal stress is slightly (7%) smaller than the input stress,
269
but the error increases rapidly when the margin for extending the FEM-grid is
270
decreased below $5\mu\text{m}$ (Fig. 4A). Total contractility and the coefficient of variation for
271
the normal stress are recovered accurately (Fig. 3D).
272

3.1.1 Effect of FEM-grid size on the stress recovery

273

pyTFM requires the user to select an area of the traction field over which pyTFM then
274
computes contractility and strain energy and draws the FEM-grid for computing
275
monolayer stresses. The size of this area influences the accuracy of the stress and force
276
measurements. Selecting an area that is too small leads to an underestimation of stresses
277
and contractility. Selecting an area that is too large also leads to an underestimation of
278
stresses. To systematically analyze which effect the size of the user-selected area has on
279
the traction and stress reconstruction, we expand the traction area and analyze the
280
average normal stress and the contractility for the synthetic test data described above
281
(Fig. 4A) and for a MDCK cell patch grown on a polyacrylamide substrate (Young's
282
modulus 49 kPa, Fig. 4B). In the case of the synthetic data, we normalize the computed
283
average normal stress and contractility to the known input stress ($1\text{ N}/\text{m}$) and to the
284
known contractility of the input traction field (600 N), respectively. In the case of the
285
experimental data, we normalize the computed average normal stress and contractility
286

to their respective maximum values as the true stress and contractility is unknown. 287

Fig 4. Effect of increasing the traction area on stress and contractility recovery. The predicted traction fields of an artificial test system (A) and a real MDCK cell patch (B). The outlines of 3 representative FEM-grids are shown on the left. The relationship between average normal stress and FEM-grid size is shown on the right.

We find that the normalized stress rapidly increases (by approximately 40%) with 288 increasing area until it reaches a maximum, after which it declines at a slower rate. The 289 contractility displays a similar initial increase but then remains approximately constant. 290 The maximum of the normalized stress occurs when the traction area just covers all 291 cell-generated tractions, including those that appear outside the cell patch. In the cases 292 of the synthetic data, the maximum is reached at a traction area expansion distance of 293 5 μm beyond the cell patch outline, whereas in the case of the MDCK cell patch, it is 294 reached at an expansion distance of 20 μm . The reason for this larger distance in the 295 MDCK data is the additional blurring of tractions introduced by the PIV algorithm 296 (whereas no PIV was needed for analyzing the synthetic data). The traction area 297 corresponding to the maximal normal stress can be regarded as the optimum, as 298 approximately 93% of the input stress is recovered. Expanding the traction area and 299 thus the FEM-grid beyond the optimum distance adds elastic material to the monolayer 300 and thereby reduces the average stress. This stress reduction, however, occurs only 301 gradually (Fig. 4B), which implies that in practice it is best to choose the traction area 302 rather generously to include all cell-generated tractions. The contractility reaches its 303 maximum values at almost the same expansion distance as the stress. Thus it is 304 possible to use the same area to accurately compute both stress and contractility. 305

3.2 Analysis of a MDCK cell-colony with pyTFM 306

In the following, we illustrate the workflow of pyTFM (Fig. 1) using a MDCK cell 307 colony as a representative example. Experimental details for this example are provided 308 in Supplementary S2 File. Two images of fluorescent beads serve as the essential input, 309 one image taken before and one image after cell removal by trypsinization of the cells 310 (Fig. 5A). pyTFM calculates the deformation field (Fig. 5B) and the traction field (Fig. 311 5C). The user then selects the area (red outline in Fig. 5) over which pyTFM draws 312 the FEM-grid and computes the contractility and strain energy (both are scalar values), 313

and the monolayer stress field (represented as a map of normal stresses (Fig. 5E)). If
314
the user optionally selects the outline of the cell patch and the boundaries of the
315 individual cells within the patch (green outlines in Fig. 5E), pyTFM also computes the
316 line tension between the cells (Fig. 5F). The program also computes a number of scalar
317 values for quantifying cellular force generation and stress distribution (Table 1).
318

Fig 5. Analysis of stress and force generation of a MDCK cell colony. A: Images of substrate-embedded fluorescent beads before and after the cells are detached by trypsinization. B: Substrate deformation field. C: Traction field. The user selects the area (red outline) over which contractility, strain energy and cell stresses are subsequently calculated. D: Image of the cell colony; fluorescent membrane staining with tdTomato-Farnesyl. E: Absolute value of the Mean normal stress in the cell colony. F: Line tension along cell-cell borders. The orange dashed line marks the outer edge of the cell colony.

The cell colony in this example displays several typical features: First, stresses and
319 traction forces are unevenly distributed across the cell colony, as indicated for example
320 by a high coefficient of variation of 0.38 for the normal component of the stress field
321 (Table 1). Second, the average line tension is higher than the average normal or
322 maximum shear stress. This indicates that, on the average, interfacial stresses between
323 cells exceed intracellular stresses. Third, normal and tensile components of the stress
324 field dominate over shear stress components, indicating that tractions are locally
325 aligned. In addition, the shear component of the line tension is considerably smaller
326 than its normal component, implying that cells in this colony pull on each other but do
327 not exert appreciable forces parallel to their boundaries.
328

Table 1. Scalar values computed by pyTFM quantifying cellular force generation and stress distribution.

Scalar Quantity	Result
Contractility	0.64 pN
Strain energy	0.11 pJ
Avg. max. normal stress	2.62 mN/m
Avg. max. shear stress	0.78 mN/m
CV normal stress	0.38
Avg. line tension	2.04 mN/m
Avg. normal line tension	1.94 mN/m
Avg. shear line tension	0.56 mN/m

4 Availability and future directions

Currently, pyTFM exclusively uses the Fourier Transform Traction Cytometry
329
algorithm [13]. This algorithm is simple, robust and well established but has a number
330
of limitations (see Section 2.2.3). However, due to the structure of pyTFM, it is possible
331
to implement alternative algorithms that address these issues with minimal changes to
332
other parts of the software. An example is the Boundary Elements Method [11] that
333
solves the inverse problem numerically in real space and allows users to set spatial
334
constraints on the tractions. This avoids the occurrence of arguably unphysiological
335
tractions outside the cell area. Another example is 2.5-dimensional Traction Force
336
Microscopy that allows for the calculation of tractions in z-directions [10]. This
337
algorithm is also necessary when cells are grown on compressible substrates and generate
338
significant z-tractions. Finally, FEM-based Traction Force Microscopy algorithms allow
339
for the analysis of cells grown on non-linear elastic substrates such as collagen [29].
340

pyTFM can be downloaded and installed from
342

<https://github.com/fabrylab/pyTFM> under the GNU General Public License v3.0.
343

Detailed instructions on the installation and usage are provided at
344

<https://pytfm.readthedocs.io/>.
345

Conflict of interest

The authors declare not conflict of interest.
347

Acknowledgements

This work was funded by the Deutsche Forschungsgemeinschaft (SFB-TRR 225, project
349
number 326998133, subproject A01, and FA 336/11-1), the Ministry of Health of the
350
Czech Republic (grant 17-31538A) and The European Cooperation in Science and
351
Technology (COST) grant CA15214-EuroCellNet (MEYS CR LTC17063).
352

5 Supporting information

S1 File. Scalar quantities used to describe cellular stresses and force generation. We discuss the definition and interpretation of the quantities that pyTFM uses to describe cellular stresses, force generation and cell-cell force transfer. 353
354
355
356

S2 File. Experimental details for analyzing the MDCK cell colony. We provide basic information on our protocols for polyacrylamide gel preparation and cell culture for the TFM analysis of the MDCK cell colony. 357
358
359

S3 File. pyTFM source code and documentation. This archive contains the pyTFM source code and documentation which includes installation and usage instructions and links to further example data sets. 360
361
362

References

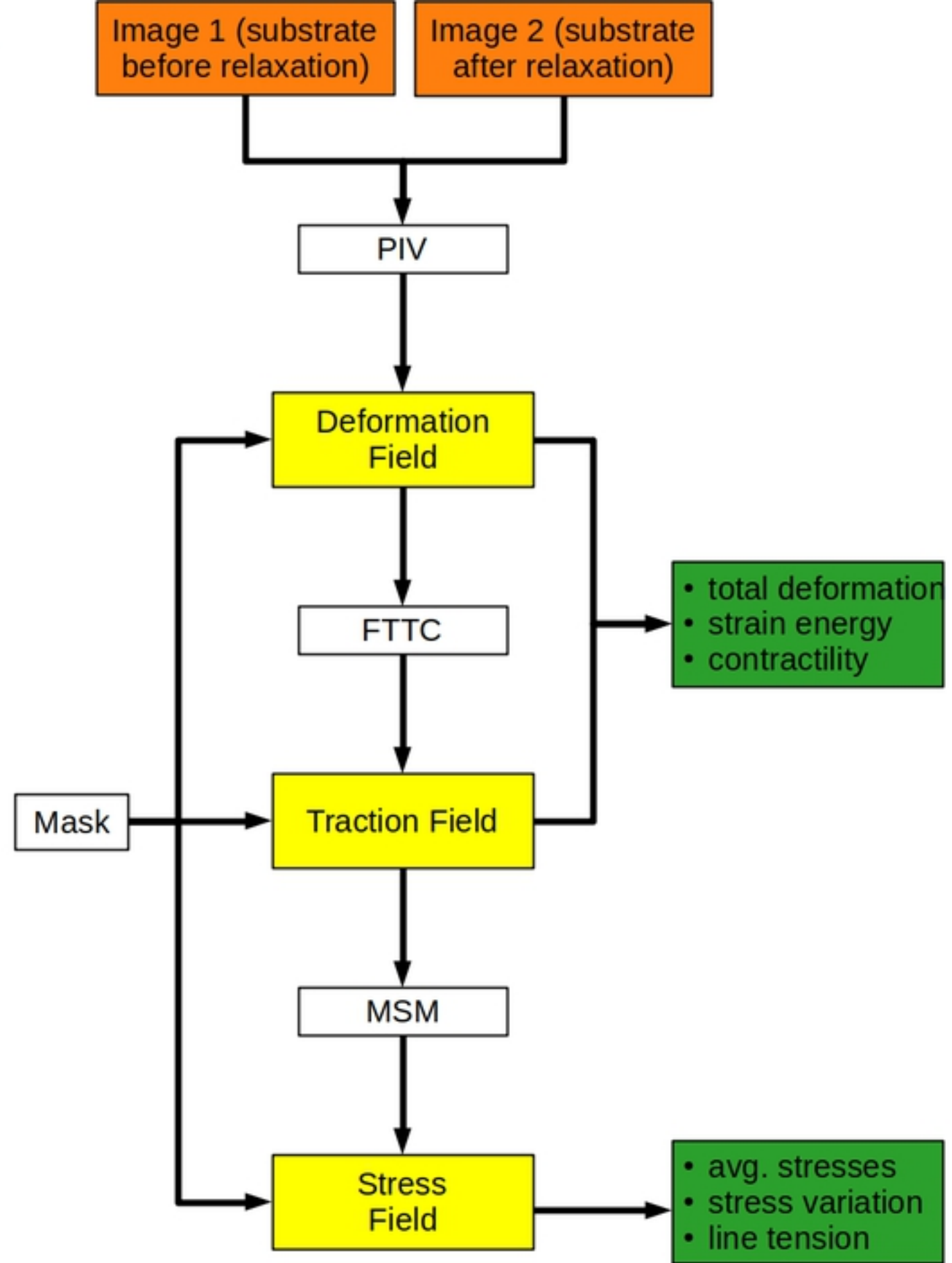
1. Pelham RJ, 1 Wang Y. Cell locomotion and focal adhesions are regulated by substrate flexibility. *Proceedings of the National Academy of Sciences*. 1997;94(25):13661–13665. doi:10.1073/pnas.94.25.13661.
2. Engler AJ, Sen S, Sweeney HL, Discher DE. Matrix Elasticity Directs Stem Cell Lineage Specification. *Cell*. 2006;126(4):677–689. doi:10.1016/j.cell.2006.06.044.
3. Steinwachs J, Metzner C, Skodzek K, Lang N, Thievessen I, Mark C, et al. Three-dimensional force microscopy of cells in biopolymer networks. *Nature Methods*. 2015;13(2):171–176. doi:10.1038/nmeth.3685.
4. REHFELDT F, ENGLER A, ECKHARDT A, AHMED F, DISCHER D. Cell responses to the mechanochemical microenvironment Implications for regenerative medicine and drug delivery. *Advanced Drug Delivery Reviews*. 2007;59(13):1329–1339. doi:10.1016/j.addr.2007.08.007.
5. Pascalis CD, Pérez-González C, Seetharaman S, Boëda B, Vianay B, Burute M, et al. Intermediate filaments control collective migration by restricting traction forces and sustaining cell–cell contacts. *Journal of Cell Biology*. 2018;217(9):3031–3044. doi:10.1083/jcb.201801162.

6. Mammoto T, Ingber DE. Mechanical control of tissue and organ development. *Development*. 2010;137(9):1407–1420. doi:10.1242/dev.024166.
7. Mark C, Grundy TJ, Strissel PL, Böhringer D, Grummel N, Gerum R, et al. Collective forces of tumor spheroids in three-dimensional biopolymer networks. *eLife*. 2020;9. doi:10.7554/elife.51912.
8. Peschetola V, Laurent VM, Duperray A, Michel R, Ambrosi D, Preziosi L, et al. Time-dependent traction force microscopy for cancer cells as a measure of invasiveness. *Cytoskeleton*. 2013;70(4):201–214. doi:10.1002/cm.21100.
9. Liberzon A, Lasagna D, Aubert M, Bachant P, Jakirkham, Ranleu, et al.. OpenPIV/openpiv-python: fixed windows conda-forge failure with encoding; 2019. Available from: <https://zenodo.org/record/3566451>.
10. Maskarinec SA, Franck C, Tirrell DA, Ravichandran G. Quantifying cellular traction forces in three dimensions. *Proceedings of the National Academy of Sciences*. 2009;106(52):22108–22113. doi:10.1073/pnas.0904565106.
11. Dembo M, Wang YL. Stresses at the Cell-to-Substrate Interface during Locomotion of Fibroblasts. *Biophysical Journal*. 1999;76(4):2307–2316. doi:10.1016/s0006-3495(99)77386-8.
12. Huang Y, Schell C, Huber TB, Şimşek AN, Hersch N, Merkel R, et al. Traction force microscopy with optimized regularization and automated Bayesian parameter selection for comparing cells. *Scientific Reports*. 2019;9(1). doi:10.1038/s41598-018-36896-x.
13. Butler JP, Tolić-Nørrelykke IM, Fabry B, Fredberg JJ. Traction fields, moments, and strain energy that cells exert on their surroundings. *American Journal of Physiology-Cell Physiology*. 2002;282(3):C595–C605. doi:10.1152/ajpcell.00270.2001.
14. Yang Z, Lin JS, Chen J, Wang JHC. Determining substrate displacement and cell traction fields—a new approach. *Journal of Theoretical Biology*. 2006;242(3):607–616. doi:10.1016/j.jtbi.2006.05.005.

15. Sabass B, Gardel ML, Waterman CM, Schwarz US. High Resolution Traction Force Microscopy Based on Experimental and Computational Advances. *Biophysical Journal*. 2008;94(1):207–220. doi:10.1529/biophysj.107.113670.
16. Tambe DT, Hardin CC, Angelini TE, Rajendran K, Park CY, Serra-Picamal X, et al. Collective cell guidance by cooperative intercellular forces. *Nat Mater*. 2011;10(6):469–475. doi:10.1038/nmat3025.
17. Tambe DT, Croutelle U, Trepat X, Park CY, Kim JH, Millet E, et al. Monolayer Stress Microscopy: Limitations, Artifacts, and Accuracy of Recovered Intercellular Stresses. *PLoS ONE*. 2013;8(2):e55172. doi:10.1371/journal.pone.0055172.
18. Tambe DT, Butler JP, Fredberg JJ. Comment on “Intracellular stresses in patterned cell assemblies” by M. Moussus et al., *Soft Matter*, 2014, 10, 2414. *Soft Matter*. 2014;10(39):7681–7682. doi:10.1039/c4sm00597j.
19. Moussus M, der Loughian C, Fuard D, Courçon M, Gulino-Debrac D, Delanoë-Ayari H, et al. Intracellular stresses in patterned cell assemblies. *Soft Matter*. 2013;10(14):2414–2423. doi:10.1039/c3sm52318g.
20. Ng MR, Besser A, Brugge JS, Danuser G. Mapping the dynamics of force transduction at cell–cell junctions of epithelial clusters. *eLife*. 2014;3. doi:10.7554/elife.03282.
21. Gerum RC, Richter S, Fabry B, Zitterbart DP. ClickPoints : an expandable toolbox for scientific image annotation and analysis. *Methods in Ecology and Evolution*. 2016;8(6):750–756. doi:10.1111/2041-210x.12702.
22. Landau LD. Theory of elasticity. Oxford England Burlington, MA: Butterworth-Heinemann; 1986.
23. Trepat X, Wasserman MR, Angelini TE, Millet E, Weitz DA, Butler JP, et al. Physical forces during collective cell migration. *Nature Physics*. 2009;5(6):426–430. doi:10.1038/nphys1269.

24. Gómez J, Guarín-Zapata N. SolidsPy: 2D-Finite Element Analysis with Python; 2018. Available from: <https://github.com/AppliedMechanics-EAFIT/SolidsPy>.
25. Lee D, Zhang H, Ryu S. In: Mondal MIH, editor. *Elastic Modulus Measurement of Hydrogels*. Cham: Springer International Publishing; 2018. p. 1–21. Available from: https://doi.org/10.1007/978-3-319-76573-0_60-1.
26. Pritchard RH, Lava P, Debruyne D, Terentjev EM. Precise determination of the Poisson ratio in soft materials with 2D digital image correlation. *Soft Matter*. 2013;9(26):6037. doi:10.1039/c3sm50901j.
27. Kim TK, Kim JK, Jeong OC. Measurement of nonlinear mechanical properties of PDMS elastomer. *Microelectronic Engineering*. 2011;88(8):1982–1985. doi:10.1016/j.mee.2010.12.108.
28. Boudou T, Ohayon J, Picart C, Pettigrew RI, Tracqui P. Nonlinear elastic properties of polyacrylamide gels: Implications for quantification of cellular forces. *Biorheology*. 2009;46(3):191–205. doi:10.3233/BIR-2009-0540.
29. Zielinski R, Mihai C, Kniss D, Ghadiali SN. Finite Element Analysis of Traction Force Microscopy: Influence of Cell Mechanics, Adhesion, and Morphology. *Journal of Biomechanical Engineering*. 2013;135(7). doi:10.1115/1.4024467.

A



B

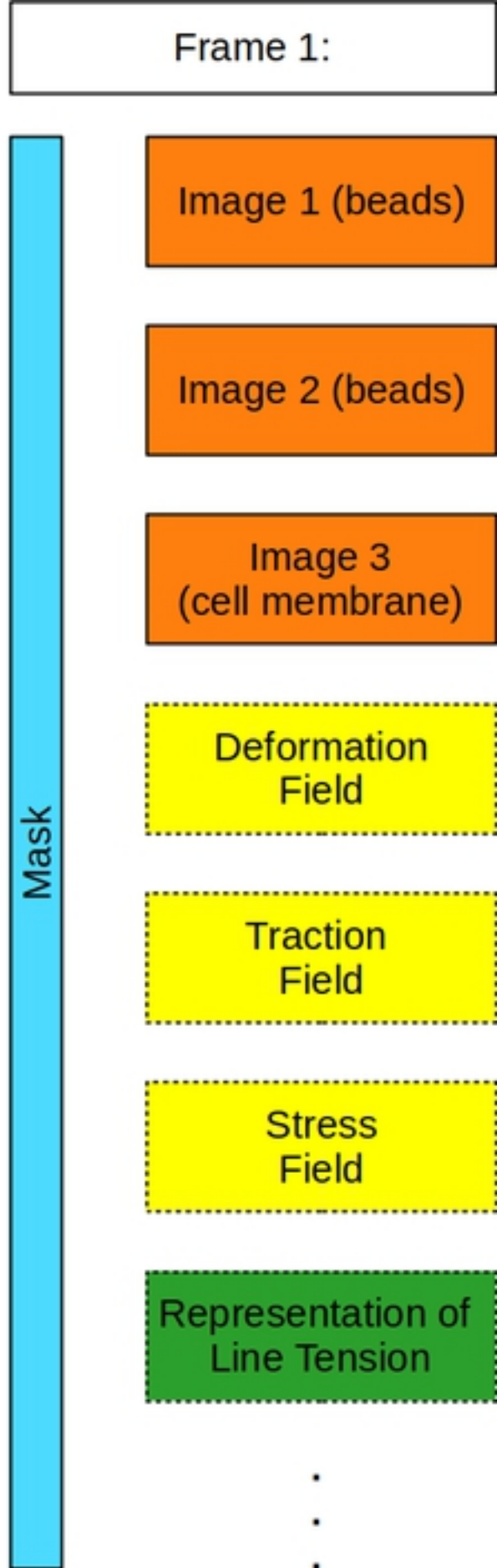
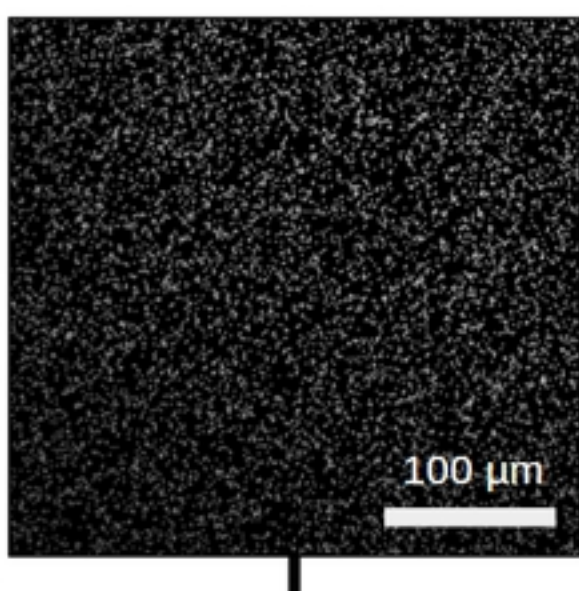
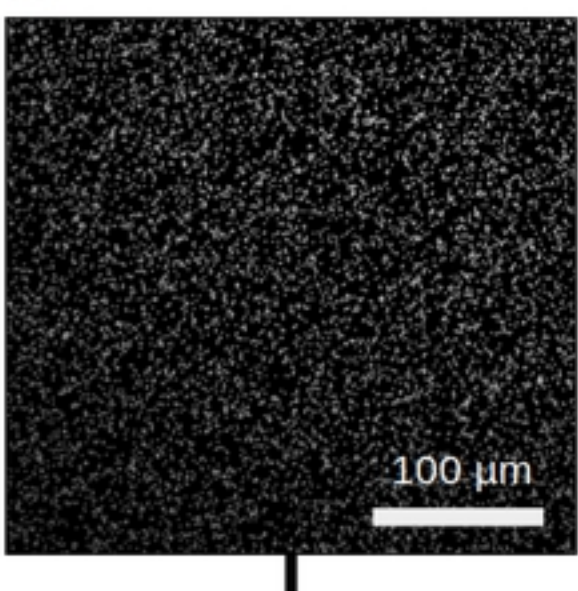
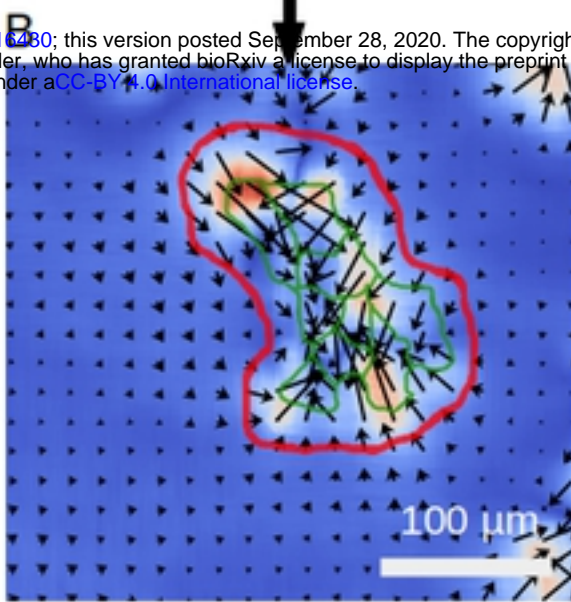


Fig1

A

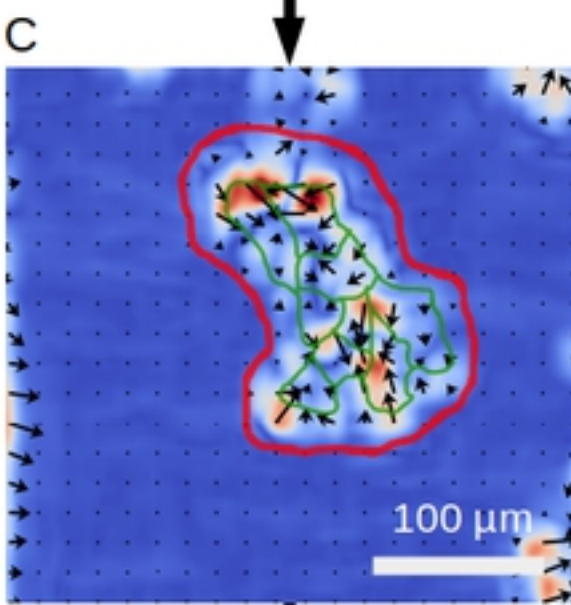


bioRxiv preprint doi: <https://doi.org/10.1101/2020.09.28.316480>; this version posted September 28, 2020. The copyright holder for this preprint (which was not certified by peer review) is the author/funder, who has granted bioRxiv a license to display the preprint in perpetuity. It is made available under aCC-BY 4.0 International license.



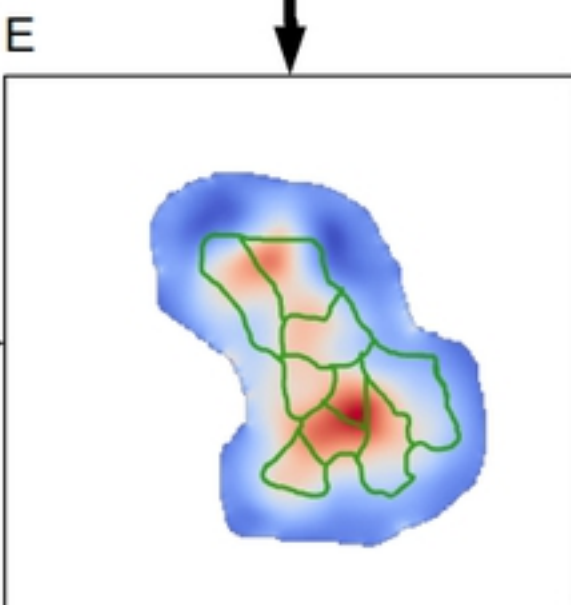
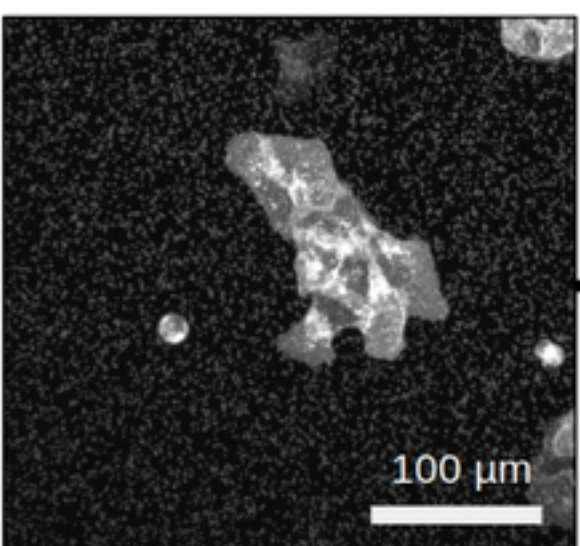
Deformation [μm]

— Traction
— Cell boundary

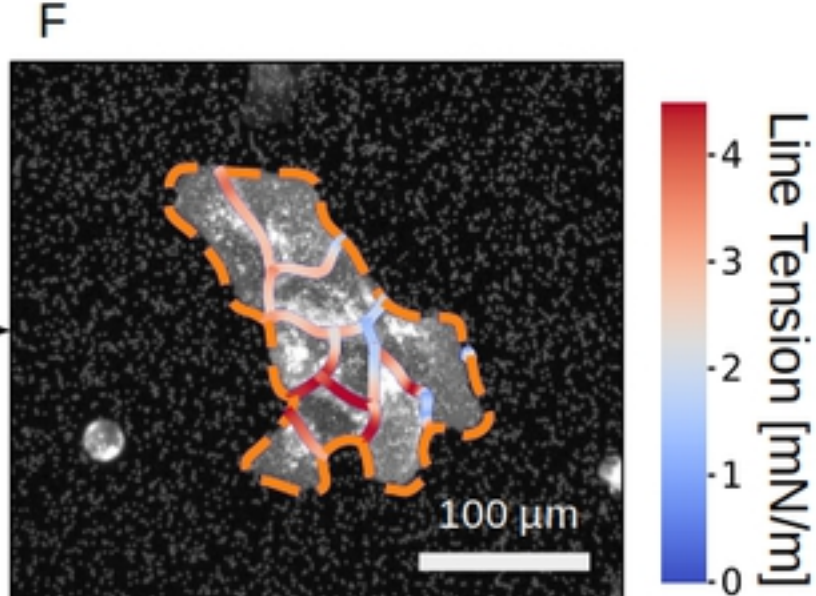


Traction [Pa]

D



Mean Normal Stress [mN/m]



Line Tension [mN/m]

Fig5



pyTFM-1.2

start

image selection

correct drift

colony segmentation

apply to

Youngs modulus [Pa]

Poisson's ratio

pixel size [μm]PIV overlapp [μm]PIV window size [μm]gel height [μm]

1

- deformation
- traction forces
- stress analysis
- force generation

2

3

current frame

49000

0.49

0.201

19

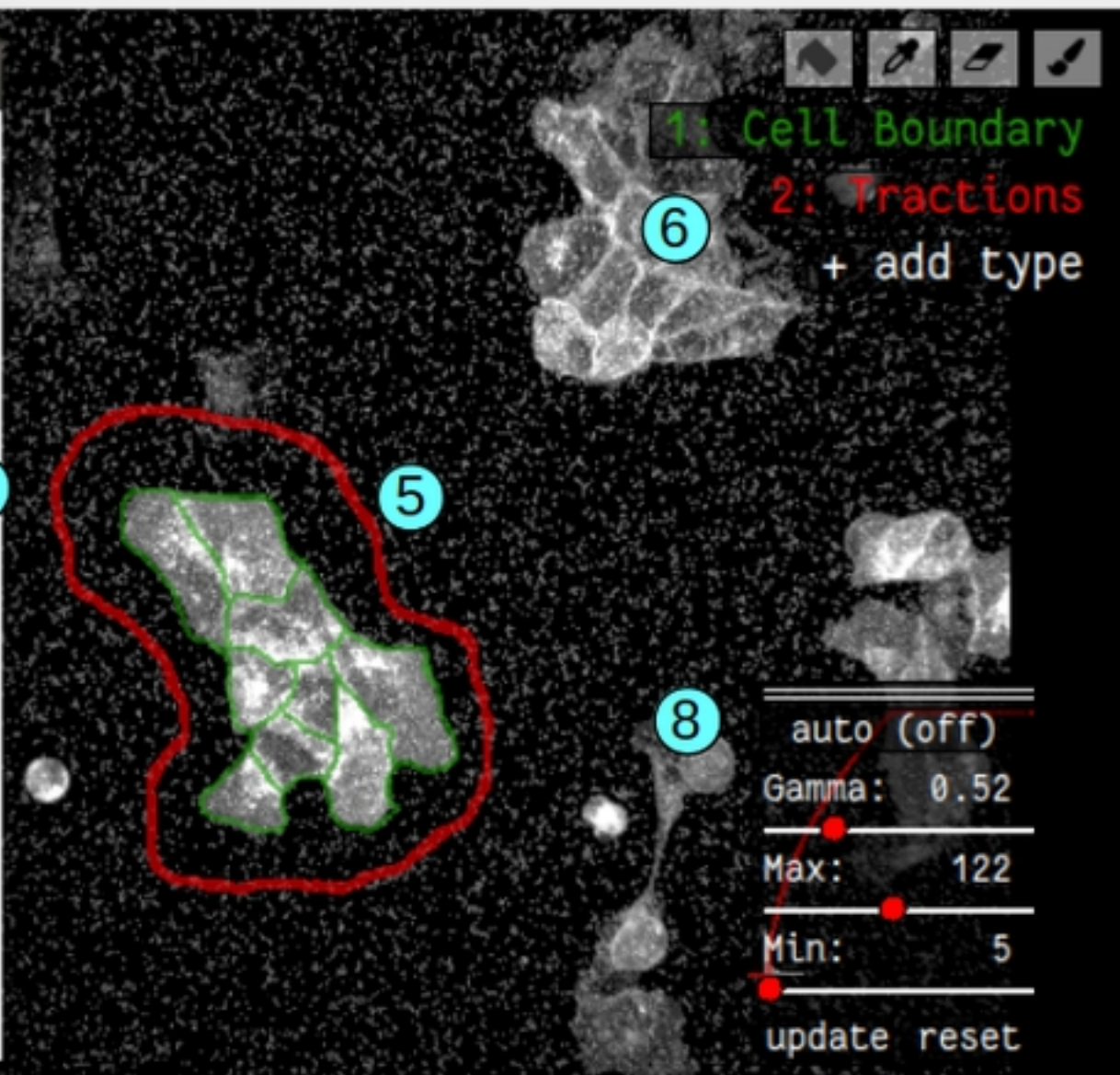
20

300



11/11 1.1fps

7



6

1: Cell Boundary

2: Traction

+ add type

5

8

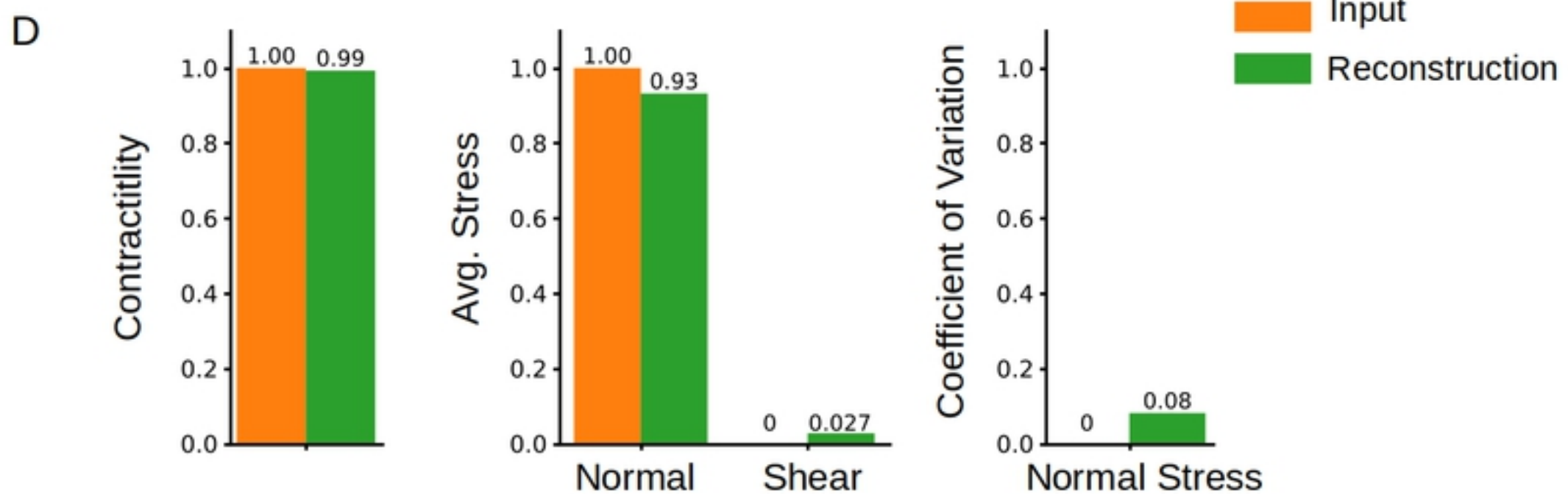
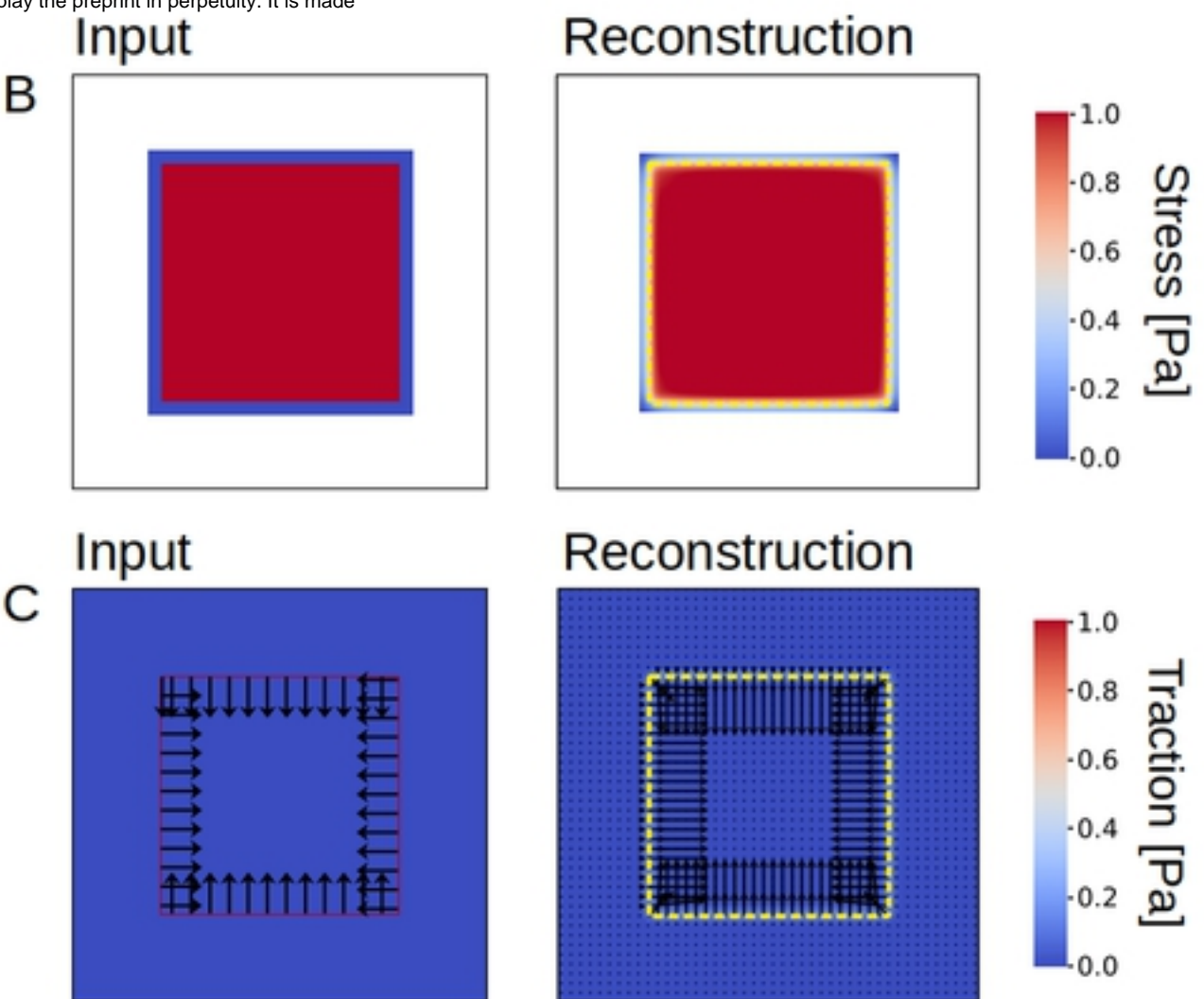
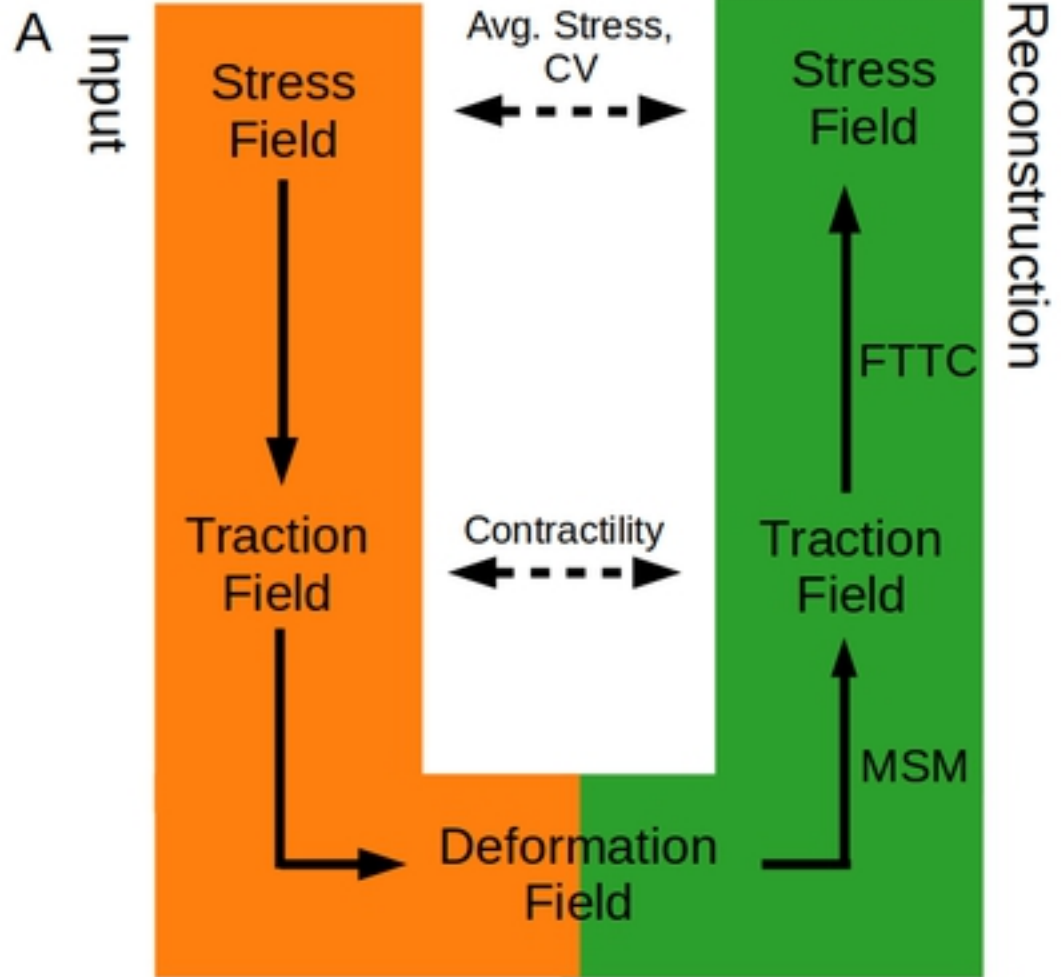
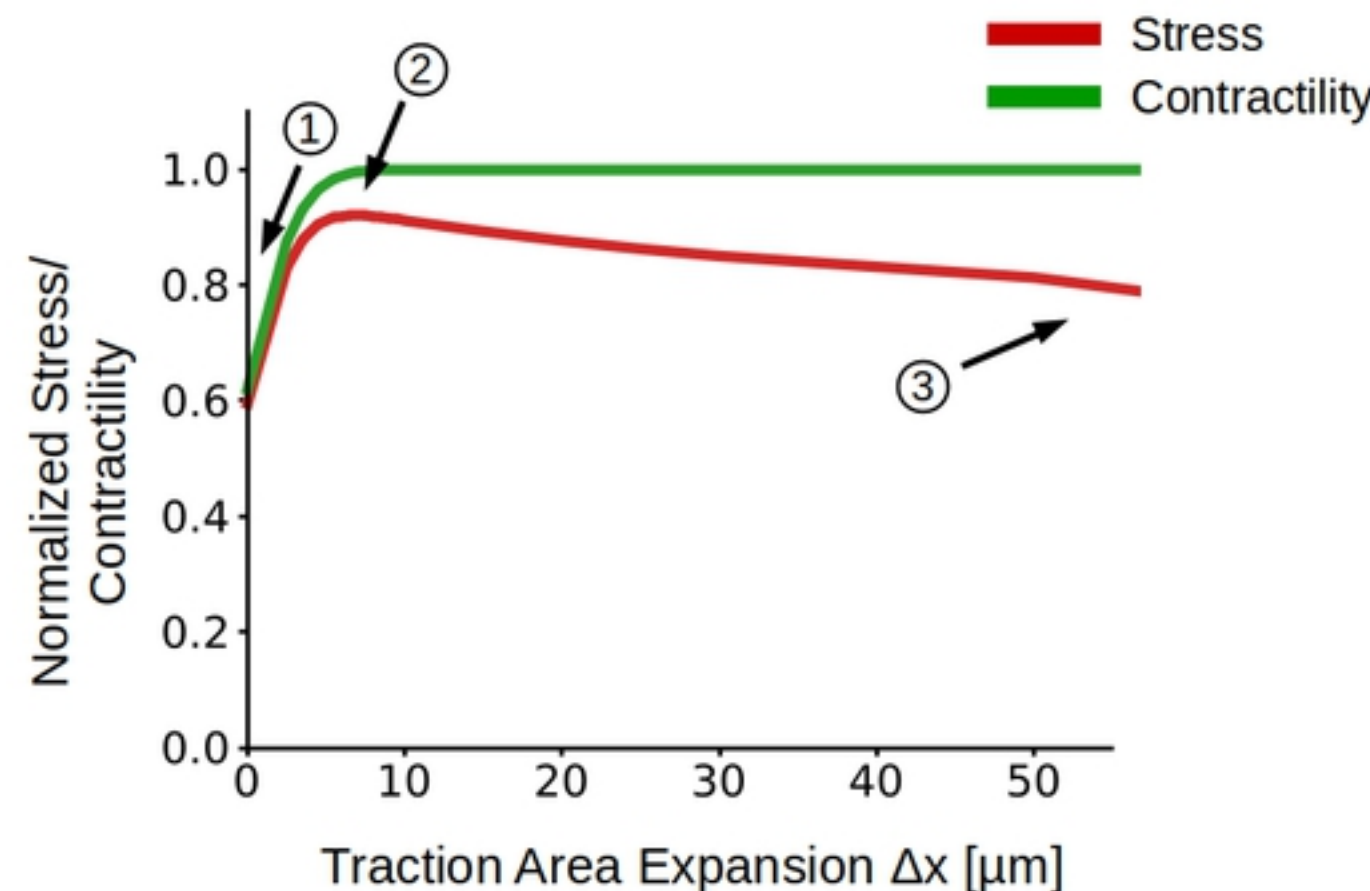
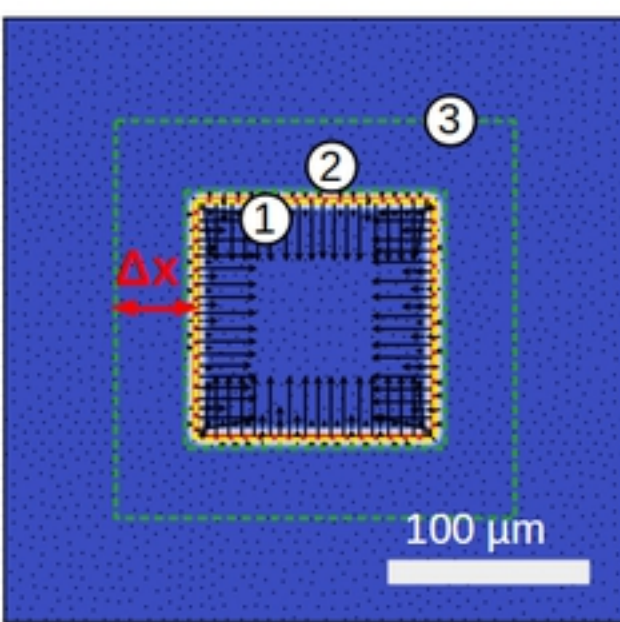


Fig1

A



B

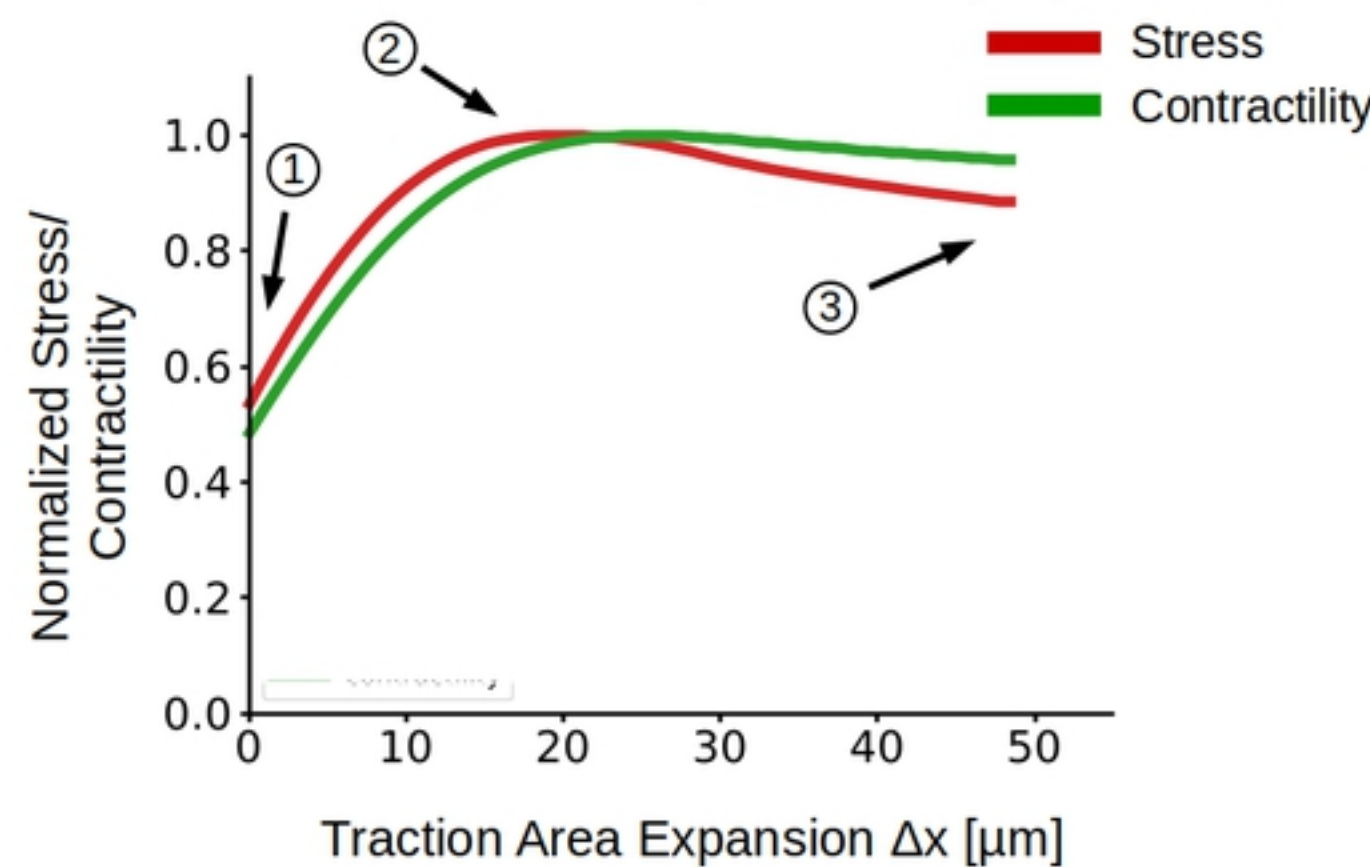
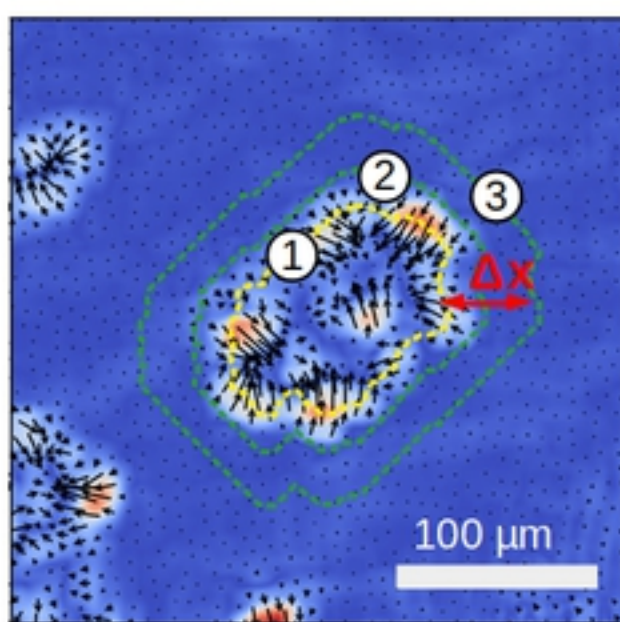


Fig4